

# Quantum light source devices of In(Ga)As semiconductor self-assembled quantum dots

Xiaowu He<sup>1</sup>, Yifeng Song<sup>2</sup>, Ying Yu<sup>3</sup>, Ben Ma<sup>1</sup>, Zesheng Chen<sup>1</sup>, Xiangjun Shang<sup>1</sup>, Haiqiao Ni<sup>1</sup>, Baoquan Sun<sup>1</sup>, Xiuming Dou<sup>1</sup>, Hao Chen<sup>1</sup>, Hongyue Hao<sup>1</sup>, Tongtong Qi<sup>1</sup>, Shushan Huang<sup>1</sup>, Hanqing Liu<sup>1</sup>, Xiangbin Su<sup>1</sup>, Xinliang Su<sup>4</sup>, Yujun Shi<sup>4</sup>, and Zhichuan Niu<sup>1, 5, 6, †</sup>

<sup>1</sup>State Key Laboratory for Superlattices and Microstructures, Institute of Semiconductors, Chinese Academy of Science, Beijing 100083, China

<sup>2</sup>School of Engineering, University of Glasgow, Glasgow G12 8LT, UK

<sup>3</sup>State Key Laboratory of Optoelectronic Materials and Technologies, School of Electronics and Information Technology, Sun Yat-sen University, Guangzhou 510275, China

<sup>4</sup>Laboratory of Solid Quantum Material Center, College of Physics and Electronic Engineering, Shanxi University, Taiyuan 030006, China

<sup>5</sup>Center of Materials Science and Optoelectronics Engineering, University of Chinese Academy of Sciences, Beijing 100049, China

<sup>6</sup>Beijing Academy of Quantum Information Sciences, Beijing 100193, China

**Abstract:** A brief introduction of semiconductor self-assembled quantum dots (QDs) applied in single-photon sources is given. Single QDs in confined quantum optical microcavity systems are reviewed along with their optical properties and coupling characteristics. Subsequently, the recent progresses in In(Ga)As QDs systems are summarized including the preparation of quantum light sources, multiple methods for embedding single QDs into different microcavities and the scalability of single-photon emitting wavelength. Particularly, several In(Ga)As QD single-photon devices are surveyed including In(Ga)As QDs coupling with nanowires, InAs QDs coupling with distributed Bragg reflection microcavity and the In(Ga)As QDs coupling with micropillar microcavities. Furthermore, applications in the field of single QDs technology are illustrated, such as the entangled photon emission by spontaneous parametric down conversion, the single-photon quantum storage, the chip preparation of single-photon sources as well as the single-photon resonance-fluorescence measurements.

**Key words:** quantum optics; quantum dots; nanowires; light sources

**Citation:** X W He, Y F Song, Y Yu, B Ma, Z S Chen, X J Shang, H Q Ni, B Q Sun, X M Dou, H Chen, H Y Hao, T T Qi, S S Huang, H Q Liu, X B Su, X L Su, Y J Shi, and Z C Niu, Quantum light source devices of In(Ga)As semiconductor self-assembled quantum dots[J]. *J. Semicond.*, 2019, 40(7), 071902. <http://doi.org/10.1088/1674-4926/40/7/071902>

## 1. Introduction

Continuously rapid development of single-photon sources (SPSs) has attracted considerable interest for both the fundamental aspects related to single photons, such as light-matter interaction<sup>[1-7]</sup> and for their significant applications in quantum information technologies<sup>[8-11]</sup>. Particularly, SPSs can potentially allow practical achievement of scalable quantum computing<sup>[12]</sup>, unconditional quantum cryptography<sup>[13, 14]</sup> and secretive quantum teleportation<sup>[15-16]</sup> systems. Typically, an ideal SPS should strictly emit photons one-by-one in terms of time series, where every photon is indistinguishable and has very high repetition rate, therefore acting as a so-called "single-photon gun". There are series of subsisted methods which can achieve the emitting of single photons<sup>[17]</sup>, where, perhaps, the simplest, the most straight-forwarded method being attenuating pulsed lasers and the generation of single photons is probable in this case<sup>[18]</sup>. The number of generated photons follows the Poissonian-statistics distribution, thus this will results in no photons, few photons or even many photons. These probable situations can give rise to baneful influence

for abundant of applications such as quantum cryptography due to possible photon number-splitting attacks ("eavesdropping")<sup>[19, 20]</sup>. As such, extensive investigations have been done for microscopic structures, in which an isolated quantum system takes effect as photonic emitting sources. Theoretically, a single quantum particle of two-level system can play as an perfect single-photon donator<sup>[21]</sup>, of which there are abundant of possible candidates, containing molecules<sup>[22]</sup>, ions<sup>[23]</sup>, atoms<sup>[24]</sup> and nitrogen vacancy centers<sup>[25]</sup>. By contrasting the low attenuated lasers and the other probable approaches, the single-photon donator derived from an isolated single quantum system can be on demand and deterministic<sup>[20]</sup>, because the single two-level system can precisely produce photons one-by-one each time. Unfortunately, the ideal isolated single quantum systems are very difficult to achieve for various reasons: can undergo photo-bleaching, or face troubles that origin from themselves extensive emitting spectra<sup>[20]</sup>. In fact, even the emitting spectra of real quantum systems are more complex than that of utopian two-level system. In view of a practical standpoint, semiconductor self-assembled quantum dots (SQDs)<sup>[6, 26-28]</sup> have high potential to offer a fascinating material system for realizing single photons<sup>[21]</sup>.

SQDs are treated as one type of atomic-like structure<sup>[29, 30]</sup>, the artificial preparation of which is realized using the strain-driven epitaxial growth mechanism. The spectrum of high-dens-

Correspondence to: Z C Niu, [zcnui@semi.ac.cn](mailto:zcnui@semi.ac.cn)

Received 1 JUNE 2019; Revised 13 JUNE 2019.

©2019 Chinese Institute of Electronics

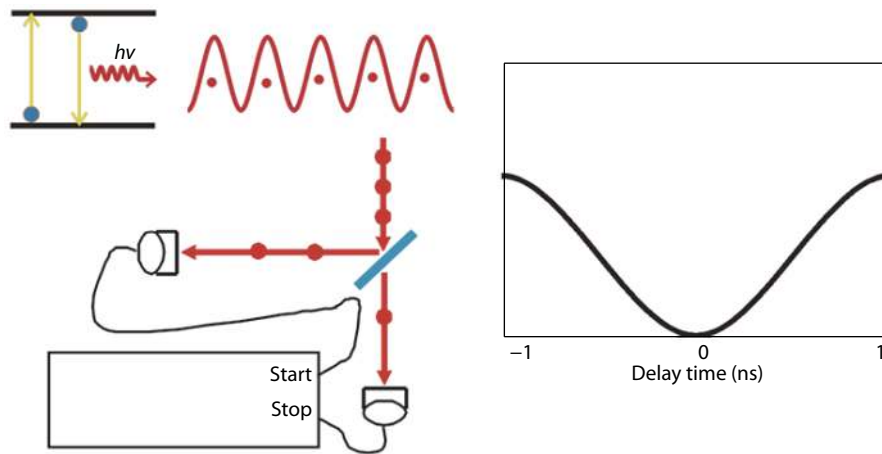


Fig. 1. (Color online) Single photons emitted from quantum 2-level transition and HBT coincidence counting test.

ity ensemble quantum dots ( $\sim 100 \mu\text{m}^{-2}$ ) looks like a continuous envelope and contains information the QD size and the continuous distribution of energy levels. The spectrum of individual low-density QDs ( $1\text{--}10 \mu\text{m}^{-2}$ ) have the isolated multi peaks, which indicates the discrete energy-level states resulted by the fluctuated QD sizes. Single QDs manifest a singlet spectrum<sup>[31]</sup>, it presents the electron-transition effect of atomic two energy levels, i.e. a single QD only emits one photon each time, displaying the antibunching effect in accordance with the time series. As shown in Fig. 1, the antibunching effect can be verified via the photon coincidence counting of Hanbury-Brown-Twiss (HBT) with 50 : 50 beam splitter (BS)<sup>[32]</sup>. Theoretically, the multiphoton probability of ideal pure single photons is zero. Self-assembled InAs/GaAs QDs achieve single photons with the following advantages. Firstly, the response of discrete local electronic states to an external field is very strong (single-exciton states generate stable single-photon current under weak excitation; the cascade-emission double-exciton states produce stable polarized correlation photon pairs under strong excitation), thus the self-assembled InAs/GaAs QDs are the current ideal materials for equipping SPSs or entangled photon sources<sup>[33]</sup>. Secondly, SQDs can be integrated into optical microcavity, diodes, waveguide and optical fiber for enhancing the directional emitting, and achieve device preparation<sup>[34, 35]</sup>. Finally, the spin states of excitons in SQDs can be regulated through varying external optical/electrical/magnetic fields and the emitted photons carry the information of spin exciton states, which is suitable for studying the quantum spin states of manipulation and realizes the ideal remote entanglement system.

Researchers have been studying QD SPSs since the single photons were observed in InGaAs QDs in 2000<sup>[36–38]</sup>. Thus far, these microstructures, consisting of GaAs/AlGaAs distributed Bragg reflector (DBR) microcavity coupled with QDs, micropillar microcavity coupled with QDs and photonic crystal microcavity coupled with QDs, have been studied as well as their related electroluminescence (EL) or photoluminescence (PL) SPS devices<sup>[2, 31, 39–47]</sup>. Domestically, our group first realized InAs QDs EL SPS operating at 77 K in 2008<sup>[48]</sup>. The optimal DBR micropillar microcavity can significantly improve the single QD emission (Purcell factor reach 6.3<sup>[38]</sup>) as the emitting wavelength exactly matches with the cavity-mode. The pulsed frequency can achieve 10 GHz (theoretically), and is expected

to improve the emitting rate of single photons. University of Wurzburg developed the EL SPSs with DBR micropillar microcavity (resonance) coupled QDs in 2010, and the related SPSs could achieve an emitting rate of 35 MHz while driven by electric pulses<sup>[41]</sup>. In order to weaken the time jitter and improve the poor coherence of QD emitting, the pulsed drive, the regulation of carrier injection and the optical resonant excitation technologies were developed by the related researchers all over the world. In 2013, the single-photon emitting time jitter was reduced by controlling the carrier injection with electric pluses in the micropillar EL SPSs<sup>[49]</sup>. Between 2012 and 2013, the deterministic emitting of indistinguishable QD single photons and entangled photon pairs<sup>[50, 51]</sup> by the pulsed resonant excitation were accomplished by University of Science and Technology of China and Stuttgart University, respectively<sup>[38, 52]</sup>. The single photons had high indistinguishability, even for two single photons of 15  $\mu\text{s}$  intervals, the coherence visibility can be as high as 92%<sup>[53]</sup>. The Raman single photons can be excited by tuning the spin exciton states of pulsed coherent light field, and both of the frequency and fluorescence lifetime are adjustable, which is convenient to expand among multiple QDs<sup>[54]</sup>. Investigation on the QD entangled photon sources were done as well during these times. Under the strain Stranski-Krastanov (S-K) mode, the morphology of self-assembled InAs QDs is asymmetry, which causes larger fine structure splitting<sup>[55]</sup> (FSS), and results in the change of degeneracy of polarization-coherent photon pairs of cascade emissions, thus they are not entangled photons. GaAs single QDs possess lower strain and higher symmetry when grown using droplet etched nanoholes growth mode, the FSS becomes very small and can be removed via optimizing the forming island or applying external strains, this GaAs single QDs are beneficial for preparing entangled photon sources with enhanced functions<sup>[28, 40]</sup>.

In farther research of QD SPSs, there are several urgent challenges to be solved: (1) preparation of individual QDs with controllable wavelength, size, morphologic of and optimization of its emitting effect; (2) the preparation of microcavity with high quality-factor ( $Q$ ), single QD emitting of microcavity enhancement and optimization of the photon extraction; (3) optimization light collection of external light paths. Significant efforts have been invested into these investigations in our team and have been rewarded with various progresses/achievements.

Table 1. Comparison of different III-V epitaxially grown QD material systems and their properties<sup>[67]</sup>.

Material system	$T_{\max}$ (K)	$\lambda$ (nm)	Comment	Ref.	
I	InGaAs/InAs/GaAs	90	~1300	~1.1–8.6	Biexponential decay [68, 69]
	InAs/GaAs	50	~850–1000	~1	
II	InAs/InP	50–70	~1550	~1–2	[71, 72]
	InP/InGaP	50	~650–750	~1	[73–76]
	InP/AlGaInP	80	~650–750	~0.5–1	[70]
III	InGaN/GaN	150	~430	~8–60	[69–79]
	GaN/AlN	~0.1–1000	~250–500	200	Lifetime increases with wavelength [80–82]

The structure of self-assembled strain-coupled bilayer QDs was firstly investigated for broadening the wavelength of GaAs-based individual InAs QDs from the traditional 0.9 to 1.3  $\mu\text{m}$ , and the 1.3  $\mu\text{m}$  SPSs of high counting rate were triumphantly obtained via integrating this structure into DBR<sup>[56]</sup>. The potential for reaching 1.55  $\mu\text{m}$  in the near future drives our current researches. The ~920 nm SPSs realized fiber output by bonding the fiber array and micropillar array, and the device stability was simultaneously enhanced<sup>[57]</sup>. Individual InAs (or GaAs) QDs and rings were respectively prepared by autocatalytic GaAs nanowires (NWs)<sup>[58]</sup>, thereby achieved both the QD single-photon emission<sup>[39, 59]</sup> and the coupling with fiber output<sup>[60]</sup>. The InAs QD emission was improved by DBR microcavity, the  $Q$  and cavity modes were observed, and the GaAs/air-gap high index contrast grating (HCG) structure was utilized to increase the output light of polarized selection. In collaboration with the University of Science and Technology of China, using the 0.87  $\mu\text{m}$  InAs QD SPSs, we successfully achieved the 100 time-mode quantum storage of deterministic single photons in the rare earth (RE) doped crystal<sup>[61]</sup>. In collaboration with the South Florida State University, the InAs QD resonance fluorescence (RF) were investigated, the resonant excitation made the two single QDs of a certain frequency emit single photons of the same frequent, however, the interference visibility was just 40% because of the charge fluctuations around QDs<sup>[62]</sup>. Furthermore, the charge fluctuation, spectrum jitter and emitting flashing could be eliminated by the additional on-band excited laser light and thus enhanced the resonance-excitation efficiency<sup>[63]</sup>. Utilizing double-color RF technique and harmonic oscillator, the QD spectrum could induce an oscillation at the half value of laser frequency, thereby the related coherence time can be longer than the natural lifetime<sup>[64]</sup>, which represents the infinite energy levels of "dressed states" ladder. We investigated the QD single photons applied in the study of quantum weak measurement after polarization encoding<sup>[65]</sup>; the application of 1.55  $\mu\text{m}$  entangled photon sources achieved via the parametric down-conversion; as well as the application of the NW QDs emitting of 775 nm single photons with the entangled fidelity of 91.8%<sup>[66]</sup>. This paper will discuss our work further as well as how it guides out future researches.

## 2. SQD materials and microcavity

### 2.1. SQD materials

Not a few materials have been taken account into the candidates of SQDs. All of them have advantages and disadvantages in terms of their single-photon properties<sup>[67]</sup>. Wavelengths ranging from the UV wavelengths to telecom wavelengths have been represented. A short list of the

main/common types of semiconductor QDs is shown in Table 1 and their main peculiarities are compared<sup>[67, 68]</sup>.

### 2.2. Microcavity coupling effect

Coupling a SQD to microcavity is very significant work due to various reasons. It consists of high quantum efficiencies, super repetition rates and outstanding single-photon indistinguishability. Typically, an unrestrained QD randomly emits single photons towards everywhere. Incorporating this QD with a microcavity will directly couple this emission into the cavity mode, which can easily achieve the optical fiber coupling or the free-space optics coupling<sup>[21, 67]</sup>. Furthermore, this related cavity mode would own a deterministic polarization, being incomparable for some linear optical quantum computing approaches<sup>[21]</sup>. These resonator structures represent via the outstanding defined spectra. This confinement causes very high  $Q$  as well as very small mode volumes ( $V_{\text{mode}}$ ). On the one hand, decoherence severely impacts the single-photon indistinguishability. On the other hand, decoherence is also a kind of significant and stubborn obstacles in achieving the quantum-information processing<sup>[21]</sup>. Many experiments are executed to work at cryogenic temperatures (typically operate at ~4 K), although this is not plenitude resolving the decoherent problems. In consequence, single QDs must possess an adequately fast photonic emitting speed (before the onset of decoherence works)<sup>[20]</sup>. In this connection, according to the Purcell effect<sup>[69]</sup>

$$F_p = \frac{3}{4\pi^2} \left( \frac{\lambda_c}{n} \right)^3 \frac{Q}{V_{\text{mode}}}, \quad (1)$$

where  $\lambda_c$  is the cavity resonance wavelength, the spontaneous emission of single QD (or atom as photon emitter) strongly changes by controlling the external dielectric environment<sup>[21, 70]</sup>.

### 2.3. Coupling QDs to microcavity for enhancing the emitting of SPSs

For single QD systems, there is merely a little of QD emitting light that escapes from sample and can be collected due to the high refractive index of III–V semiconductors. As shown in Fig. 2, contrasting high refractive index materials such as GaAs ( $n_1 = 3.59$ ) with low refractive index materials such as air ( $n_2 = 1$ ), the inward angle of total reflection is less than  $\theta_c$  ( $\theta_c = \sin^{-1}(1/3.59) = 17^\circ$ ). Namely, if the incident photons arrive at the surface of semiconductor, there will be nothing detected by probes besides the total reflection occurs in devices. The solid angle of photons far away from sample is

$$\Omega = 2\pi(1 - \cos\theta) = 2\pi \left[ 1 - \left( 1 - 1/2n^2 \right) \right] = \pi/n^2, \quad (2)$$

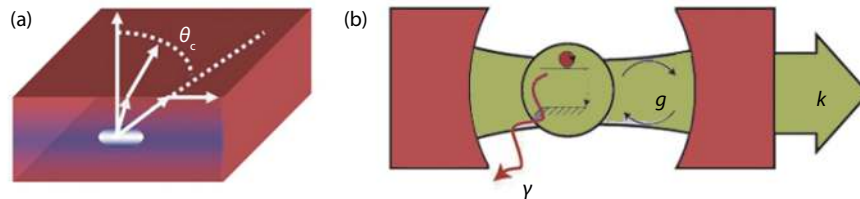


Fig. 2. (Color online) Schematic diagram of (a) inward total reflective angle and (b) the interaction between atom and microcavity<sup>[75]</sup>.

Moreover, the efficiency of the collected photons is

$$\eta = \Omega/4\pi = 1/4n^2. \quad (3)$$

The  $\eta_{\text{GaAs}}$  is only  $\sim 2\%$ , before taking into account the following factors, such as surface roughness,  $\theta < \theta_c$ , absorption of materials and so on. Therefore, it is important to improve the collected efficiency of photons. Generally, an optical microcavity is used in enhancing the collected efficiency of photons in experiment. Optical microcavity is a kind of micro resonant cavity that possesses a matched length comparing with photonic wavelength at one-dimension (1D) orientation at least. There is characteristic of both the pattern of small volume ( $V$ ) and high  $Q$ , simultaneously. The  $Q/V$  of optical microcavity is much larger than the ordinary optical resonant cavity, which leads to the variation of photonic density states<sup>[67]</sup>.

The traditional optical microcavity is divided into four categories that include Fabry-Pérot (F-P) cavity<sup>[71]</sup>, the Whispering-Gallery (W-G) cavity<sup>[71]</sup>, the photonic (P-C) crystal<sup>[71]</sup> and the surface plasmonic polariton (SPP) cavity<sup>[43, 67]</sup>.

### 3. In(Ga)As single QD single-photon sources and devices

#### 3.1. Emitting-wavelength scalability of In(Ga)As single QDs

InAs single QDs form at near critical point to island formation, when InAs deposition deviate from that point, QDs either form with high-density or not form QDs at all. Although we have controlled over the growth via MBE instruments, the critical point to island formation varies with the temperature drift, the flux instability, the vacuum background float and the thermal conductivity of different molybdenum pallet. Consequently, it is difficult to prepare single QDs according to fixed header parameters. Gradient flux can broaden the parametric tolerance of indium deposition, which ensures the existence of single QD area on a wafer. The method of *in situ* desorption can exactly monitor the critical indium deposition ( $\theta_c$ , the sacrificial QD layer subsequently desorbs by *in situ* annealing) of the island formation of sacrificed layer each time by reflection high-energy electron diffraction (RHEED), and then ensures the optimal indium deposition of  $\theta$  to grow the active QD layer. Due to the similar QD growth conditions for both the sacrificial layer and the active layer, the optimal indium deposition of prepared QDs almost keeps conformance, the ratio of  $\theta/\theta_c$  is usually independence of temperature and fluxes. According to the experimental experiences and statistical analysis, the stable critical parameters of island formation were found, i.e. the single QD regular criterion  $\theta_c = 1.7\text{--}2.31$  monolayer (ML) and the steady parameters of  $\theta/\theta_c$ <sup>[72]</sup>. The singlet spectra of 900–935 nm wavelength band correspond to the emitting

of 7–8 nm height single QDs. The distribution of single QDs on a wafer depends on the temperature distribution. The normal criterion of island formation is beneficial to decrease the failure rate of single QD preparation and saves high purity sources and machine time.

In fiber quantum communication, it is necessary to develop 1.31 and 1.55  $\mu\text{m}$  SPSs, whereas, the emitting wavelength of individual InAs/GaAs SQDs usually locates at  $\sim 0.9 \mu\text{m}$ . We introduced the strain-coupled bilayer InAs QD structure for the first time to ease the strain accumulation and increase the upper size limit of faultless emitting-light QDs. We broadened the emitting wavelength of InAs/GaAs single QDs to 1.3  $\mu\text{m}$  (Fig. 3) and improving the emitting efficiency by optimizing QD density, growth temperature and introducing charge exciton states. The current work indicates high promises for expanding emitting wavelength to 1.55  $\mu\text{m}$ . After introducing the AlGaAs-barrier layer, the emitting wavelength of InAs/GaAs single QDs could blue shift to 0.84–0.86  $\mu\text{m}$ . The micro-PL spectrum of 1.3  $\mu\text{m}$  single QDs demonstrated the emitting light of single excitons.

The wavelength scalability of QDs can be realized by adding hydrostatic pressure on diamond anvil cell (DAC). On the pressure of 6.58 GPa, the emitting wavelength of 1.3  $\mu\text{m}$  QDs blue shifts to 0.9  $\mu\text{m}$  and  $g^2(0)$  is less than 0.3, which represents the single-photon properties of QDs<sup>[73]</sup>. It provides a new method of tuning QD emission wavelength in a broaden range, which is different from the current methods such as bias-pressure adjustment and temperature adjustment.

#### 3.2. High Q DBR microcavity enhancing the emitting of In(Ga)As single QDs

Batches of GaAs/AlGaAs DBR micropillar microcavities can be prepared together by combining optical exposure and ion etching on a single wafer. Several factors should be considered mainly: (1) matching with the emitting wavelength of single QDs (the precise calibration of DBR thickness and cavity mode); (2) the appropriate upper and down number of DBR pairs; (3) the suitable diameter and shape of micropillar; (4) the fine smoothness of side wall after optimizing the etching processes. The  $Q$  varies from hundreds to thousands with different parameters of geometrical technologies. There is multiple-step W-G cavity besides the main F-P cavity mode, when the micropillar diameter surpasses 2  $\mu\text{m}$ . The  $Q$  of smooth sidewall W-G is as high as 17 000<sup>[74]</sup>. The elliptical micropillar can realize a splitting of anisotropic modes, which is advantageous for polarization excitation. The DBR structure with upper 8-pair to down 20-pair was adopted to acquire the smooth sidewall forward and reversed tapered micropillars by optimizing the deep etching process (Fig. 4). The micropillar  $Q$  of 920 nm wavelength is in the range of 1063–8840 (The measured  $Q$  of cavity-mode spectrum is in the range of 1063–5240), and the

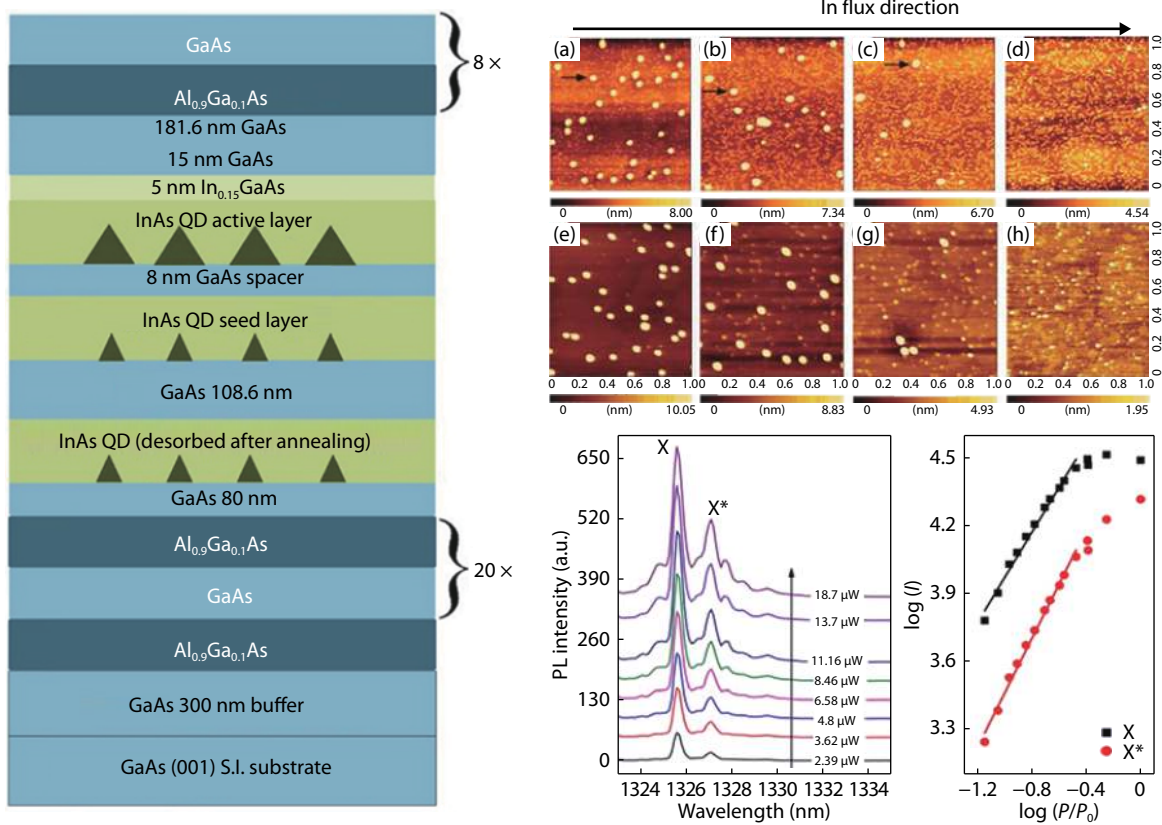


Fig. 3. (Color online) Strain-coupled InAs/GaAs single QDs emit at  $1.3 \mu\text{m}$ <sup>[56, 76]</sup>.

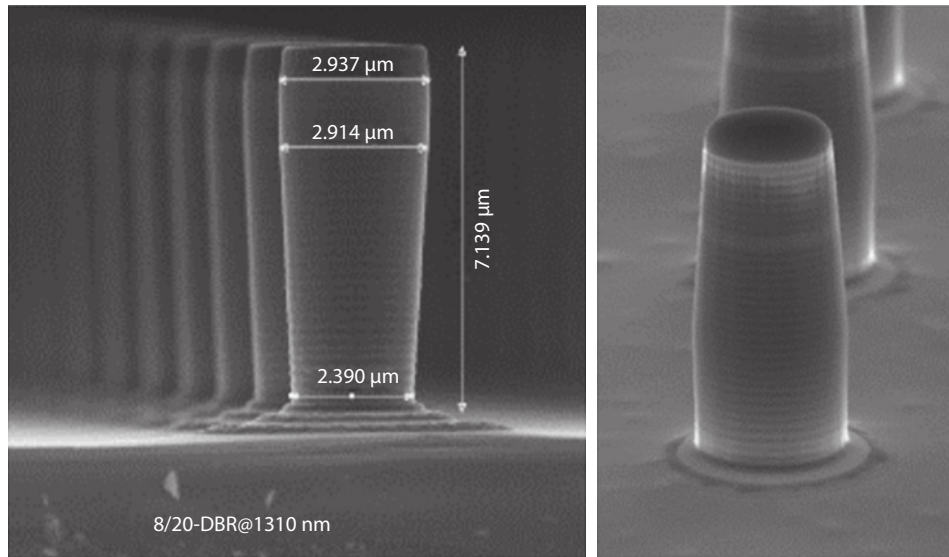


Fig. 4. (Color online) Forward and reversed tapered micropillars with smooth facet<sup>[56]</sup>.

spectrum of high  $Q$  is difficult to examine due to the weak sign. The  $Q$  of  $1.3 \mu\text{m}$  wavelength micropillar is in the range of 300–1890 (the spectrum of 300  $Q$  cavity mode is measured<sup>[39]</sup>).

The SPSs of high counting rates were obtained via adjusting the resonance between cavity modes and single QDs. In view of  $1.3 \mu\text{m}$  wavelength strain-coupled bilayer InAs single QDs, the saturated counting rates of single photons arrive at  $60000 \text{ s}^{-1}$  by connecting avalanche photon detector (APD) with HBT test header, the emitting speed before arriving at the first lens is calculated to be 3.45 MHz, and the  $g^2(0)$  is as low as

$0.14$ <sup>[39]</sup> (Fig. 5).

Due to the high refractive index, the total surface reflection of GaAs is high while the efficiency of emitting is low. We found that integrated GaAs/air-gap HCG on DBR microcavity surface structure that could improve the vertical emitting efficiency and realize the polarization of emitting of single photons. Utilizing the ICP etching in grating graphics, the selective etchant flows through the grating gap into AlGaAs buried layer for corrosion, thus the HCG forms. This complex 3D microcavity has large cavity volume, relaxed process tolerance

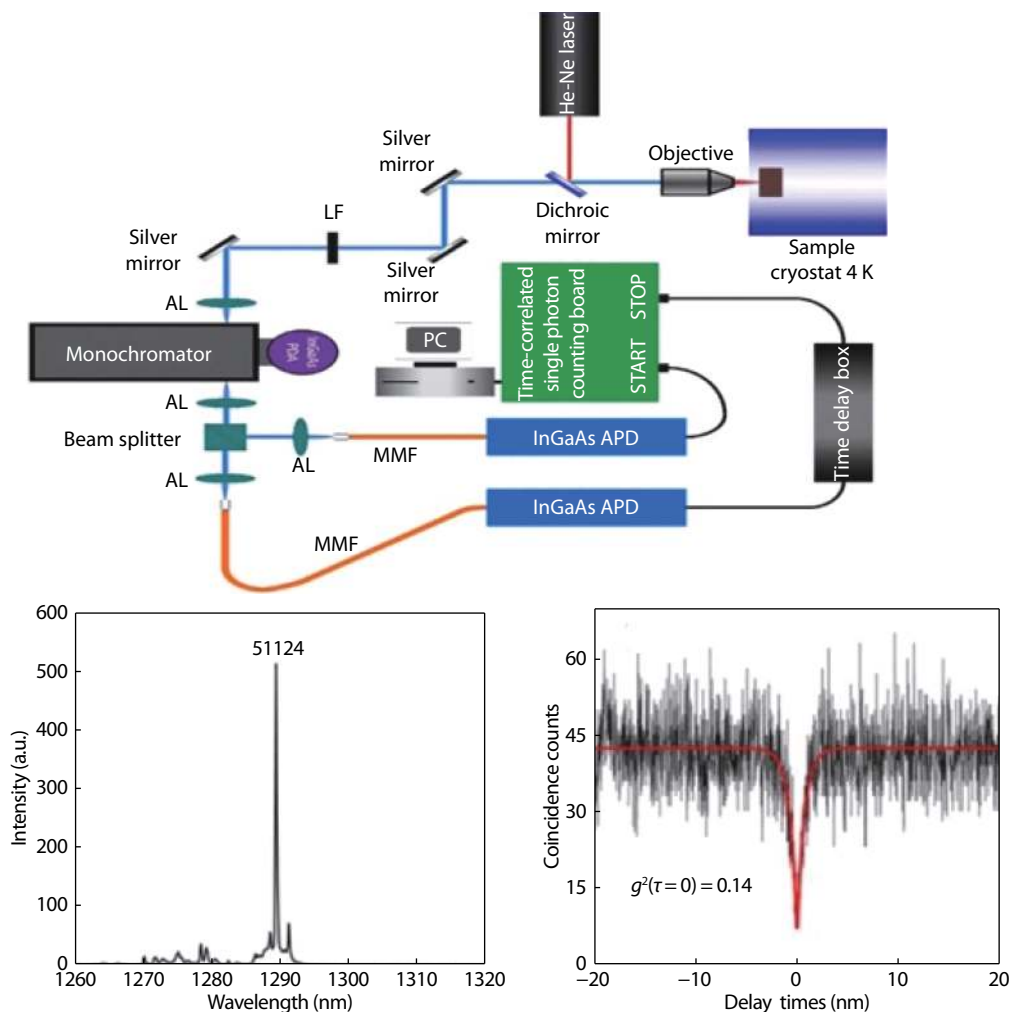


Fig. 5. (Color online) Test of 1.3  $\mu\text{m}$  micropillar coupled QD SPSs<sup>[56]</sup>.

and easily couples with single QDs.

Confocal optical path of spatial resolution is applied in characterizing the QD single photons. The lights of PL excitation and PL emission were both converged by objective lens. The size of light spot dominates the spatial resolution of  $xy$  in-plane, and the space filtering of  $z$ -axis takes place in the pinhole of back-end. There is a free-space confocal optical path (Fig. 5, the pinhole is replaced by the slit of spectrometer) and an optical fiber confocal optical path (the pinhole is replaced by the optical fiber core). The single photons can be extracted from the spectra of substrate layer, wetting layer and/or QD layer by grating or filter lens, then they enter APD counting through HBT device after the multi-mode fiber coupling. The efficiency of optical path is severely affected by the stability of system and the precision of focusing. The APD collection efficiency of single photons is generally between 1%–3% through the free-space confocal optical path (Fig. 5). The APD collection efficiency of single photons can arrive at about 7% by optimizing fiber confocal optical path with precise focusing and positioning of device<sup>[38]</sup>.

### 3.3. QD growth and single-photon emission in NWs

There are many advantages to growing individual QDs on NWs. The NW growth possesses the high tolerance for lattice mismatch; diversified NWs, such as GaAs, InAs, InP, GaN and InSb, can simultaneously grow on a substrate, and the full-wavelength band QDs can be achieved based on NWs. The spa-

tial discreteness of NWs is beneficial to the control of QD density. The light field of NWs has the distribution of broadband mode (axial waveguide mode and sectional W-G waveguide mode), which can strengthen the QD emitting of different wavelength band and make the light to firmly output from the top of the NWs. The no defect QDs of steep-interface hetero-junction can be obtained. The gas-liquid-solid growth of NWs requires droplet catalysis, and Ga droplet is suitable as catalyst because of its no-pollution. The density-controllable GaAs/AlGaAs core/shell-structure NWs of uniform length and orientation can grow on Si substrate by changing the epitaxial rate, time, arsenic (As) pressure, deposition temperature and AlGaAs capping thickness as well as the Y-type bifurcated NWs can be prepared via twice Ga-droplet-catalyzed epitaxy. The InAs/GaAs and GaAs/AlGaAs individual QDs can grow on the sidewall of NWs after excessive InAs and GaAs deposition (Fig. 6). The nucleation progresses of QDs are affected by the surface strain. InAs QDs preferentially grow in the bifurcated position of NWs, because the GaAs/AlGaAs interface strain is larger. GaAs QDs are formed on the sidewall of NWs, and these QDs can emit single photons. The spectrum of InAs/GaAs single QDs presents fine and sharp peaks at 4.2 K, the linewidth is only 101  $\mu\text{eV}$ , and  $g^2(0)$  is as low as 0.031<sup>[30]</sup>. The crystal quality of AlGaAs/GaAs single QDs is excellent, the anti-bunching light can be detected at 77 K,  $g^2(0)$  is just 0.18<sup>[56]</sup>, and the microcavity enhancement can be observed. The struc-

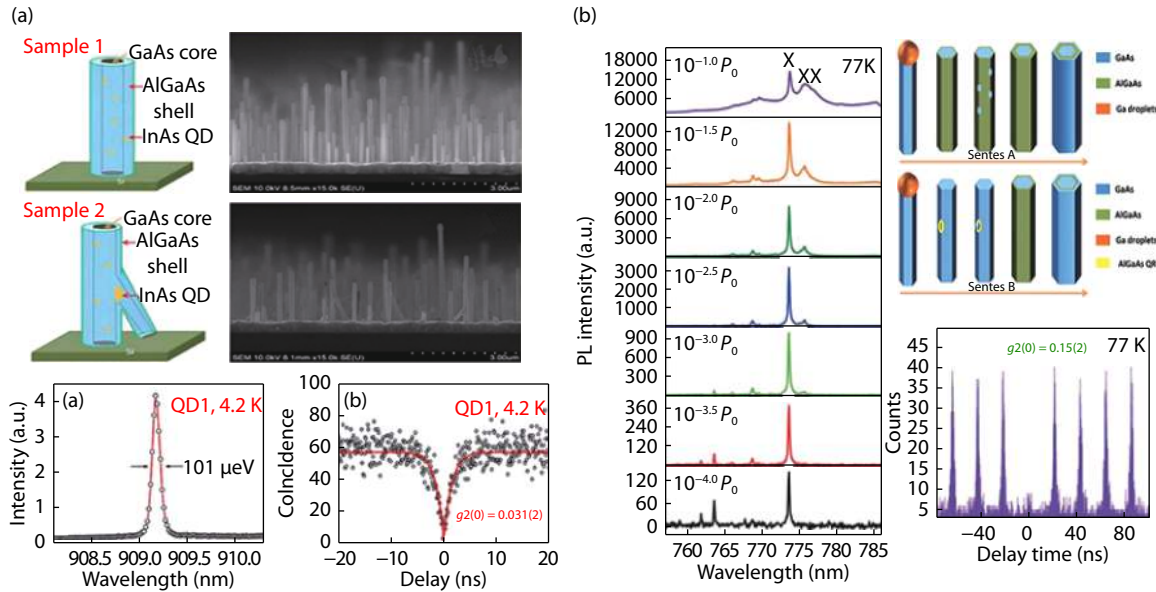


Fig. 6. (Color online) InAs (a), GaAs (b) QDs on droplet self-catalyzed NWs and their exciton emission<sup>[39, 59]</sup>.

tures of GaAs quantum rings and ring midpoints are prepared on the sidewall of GaAs NWs by tuning growth parameters, thereby the QDs density and morphology can be controlled. The emitting light of quantum rings is measured by 10 K PL spectrum and 77 K cathode luminescence (CL) spectrum and the spectra show sharp peaks, the interval is among 1–3 meV and the narrowest width is only 578  $\mu\text{eV}$ , which indicate the quantum properties of ring electron states<sup>[58]</sup>.

### 3.4. Optical fiber coupling output chip of QD single-photon emitting

Directly using the abovementioned microcavity with optical fiber can guarantee the stability of system and make the related characterizations to be simple, which would enable the single photons to go out of the laboratory. Smoothly laminating the end face of fiber with the light-output side of microcavity, the collected efficiency of emission light depends on the numerical aperture (NA) of fiber and alignment accuracy. The fibers of excited light (650 nm) and emitted (980 nm) light connect with one path of fiber probe via the fused fiber wavelength-division multiplexer (WDM), the single QDs on the sample surface are searched by near-field scanning, and the real-time characterization proceeds after the fiber of emitting connected with fluorescence spectrometer. The sample tank is filled with liquid nitrogen to cool luminescent QDs while the test is on line. The coupling adhesion is finished between single QDs and fiber after the volatilization of liquid nitrogen. This method is applied to realize the single-photon fiber output of NWs<sup>[60]</sup> (Fig. 7).

Owing to the small end face of optical fiber, this adhesive method almost inevitably slopes between fiber and QD chip and affects the emitting collection. Thus, the micropillar array and the single-mode fiber array are adhered by the way of blind alignment, because the fiber array offers the flat end face as the matched adhesive facet of chip and the micropillar cycles ensure the existence of micropillar under each fiber. The single-photon fiber output of 920 nm QDs is realized successfully, the single-photon counting rate of output end arrives at the highest frequency of 420 kHz and  $g^2(0)$  is as well as

0.02, which imply that the maximum estimate of the receiving single-photon counting rate of fiber coupling surface reaches 1.8 MHz<sup>[57]</sup> (Fig. 8). Combining with the 25% collected efficiency of optical fiber, the 30% filter efficiency of back end and the overall single-photon collecting efficiency of optical path is up to the highest value of 1.7%, which is closed to that of confocal optical path.

### 3.5. Resonance fluorescence of In(Ga)As single QDs

Resonant excitation can improve the coherence of the QD single photons, while the difficulty is keeping the emitting light apart from exciting light completely. Normally, the vertical QD emitting and collection under lateral excitation can be applied to keep their separation. As shown in Fig. 9, we studied QD RF in cooperated with Muller's group in University of South Florida<sup>[62]</sup>. Zooming two single QDs of similar emitting wavelength into an approximate spatial distance of 40  $\mu\text{m}$ , the two single QDs would emit the single photons of identical frequency by tuning the resonant excitation. The emitting interference between the two single QDs was supervised and the interference visibility was only 40% because the fluctuation of charge occupy around single QDs caused the frequency jitter of QD emitting. Another on-band excited laser light was used to fill the charge state, which could eliminate the charge fluctuation, the spectral jitter and the flashing light<sup>[63]</sup>. We further studied the influence of the coherent and incoherent scattering composition in RF, the pure coherent scattering and the phase-loss decoherence under weak excitation, the jitter of spectrum, correlation function and the phase coherence<sup>[63]</sup>. We firstly studied the resonant scattering of two beams of independent tunable continues wavelength (CW) laser light in InAs QDs. In the experiment of double color RF, the extra light field gave rise to oscillation at the half difference of laser frequency and harmonic oscillator frequency, the oscillating time stayed longer than that of nature life, which illustrated that the "dressed state" ladder in each group included an infinite number of energy levels. The spectrum and the second-order correlation functions could be reappeared by Bloch equation and quantum-regression theory<sup>[64]</sup>.

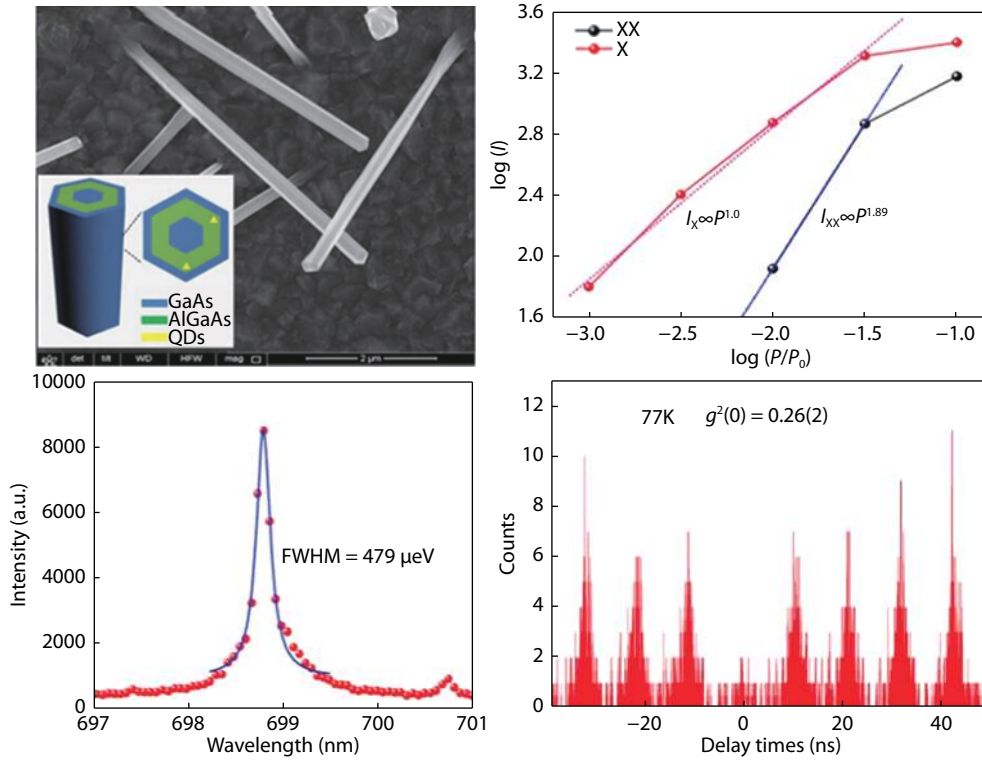


Fig. 7. (Color online) Direct fiber extracted AlGaAs/GaAs QD SPSs<sup>[60]</sup>.

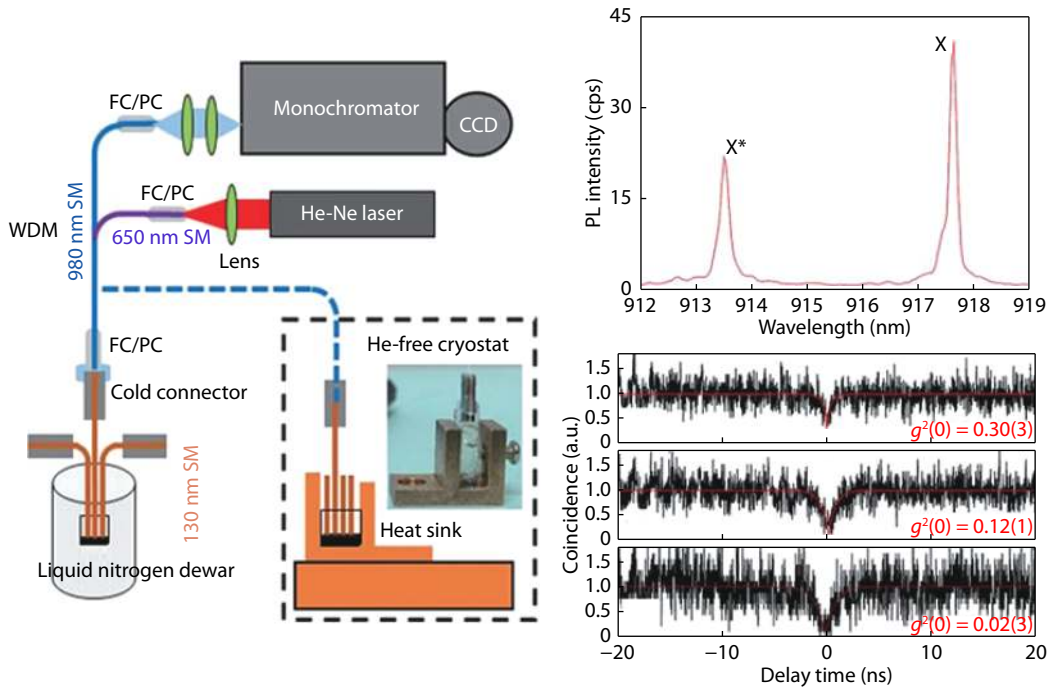


Fig. 8. (Color online) Direct fiber extracted InAs/GaAs QD SPSs<sup>[57]</sup>.

### 3.6. Entangled photon emission by the spontaneous parametric down-conversion of QD single photons

We explored the achievement scheme of entangled photon pairs derived from the single photons through nonlinear crystal QD under spontaneous parametric down-conversion (SPDC). The emitting wavelength band of NW QDs locates at 650–780 nm. The exciton emitting peak of NW QDs

centered at 775 nm was converted into the entangled photon pairs of 1.55 μm by SPDC through the ultraviolet-light (UV-light) pulsed excitation, the collection of confocal light path, the polarization and the crystal waveguide of periodically poled lithium niobate (PPLN). The nonlinear conversion efficiency of PPLN waveguide is very high, the wide band of 770–780 nm and the tunable output wavelength band of 1550–1600 nm can become real by tuning temperature pre-



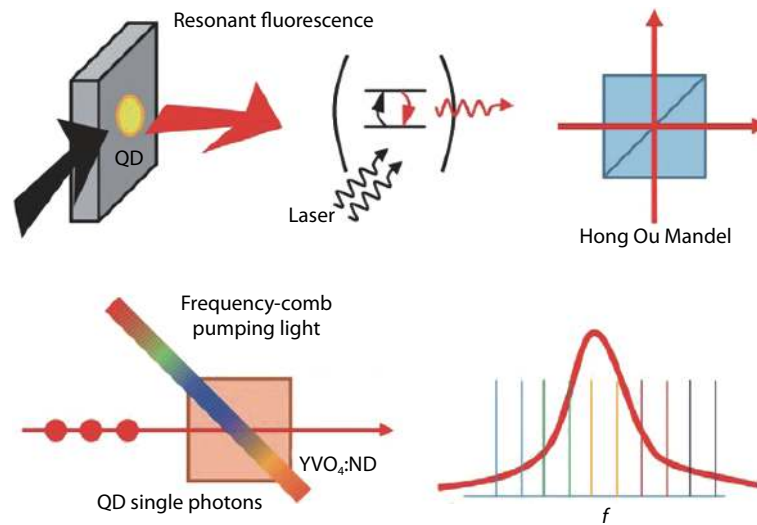


Fig. 9. (Color online) QD RF and single-photon quantum memory.

cisely, and the fidelity of the entangled photon pairs arrives at 91.8%<sup>[66]</sup>.

### 3.7. QD single-photon solid-state quantum storage and quantum measurement

Entangled distribution is the core technology to construct the quantum network. The directly entangled distribution can only reach hundred kilometers magnitude in channel due to the channel-transmission loss. The long-distance entangled distribution needs the quantum repeater technology based on single-photon quantum storage and two-photon Bell measurement. So far, the program of quantum repeater verified by experiment are all based on the probabilistic quantum light sources (low generated probability of photons and existing multiphoton pulses). The distribution time of long-range entanglement is estimated to be above the minute magnitude. In cooperation with University of Science and Technology of China, we utilized the self-assembled QDs to generate the deterministic  $0.87 \mu\text{m}$  single photons. The single photons passed through fiber into  $\text{Nd}^{3+}$ -doped  $\text{YVO}_4$  crystal that located at another optical platform about 5 m away, the highest 100-time models of deterministic single photons and the minimum of 1-time model quantum storage were realized, thus the number of models got to the highest level<sup>[61]</sup>. The distributed time of long-distance entanglement was expectedly shortened into the magnitude of millisecond levels by combination of deterministic quantum light sources and multi-mode quantum reservoirs. The single-photon wavelength ( $\sim\text{GHz}$  line-width) of QDs would resonate with the absorbed wavelength (879.7 nm,  $\sim 100 \text{ MHz}$  line-width) of  $\text{Nd}^{3+}$  ions by tuning the temperatures. In order to enhance the adsorbed intensity, we also introduced the pumping light of periodic frequency-modulation 879.7 nm in  $\text{YVO}_4$  crystal, the generated atomic frequency comb broadened the absorbed spectrum in  $\text{Nd}^{3+}$  ions (Fig. 9).

We collaborated with University of Science and Technology of China, the QD single photons were firstly encoded after polarization and then was used to validate the compromise relationship between the quantum-state measurement and the probability of reversible recovery under weak measurement condition<sup>[65]</sup>. The experiment is very significant for the ap-

plication of QD single photons in quantum measurement and quantum communication.

## 4. Summary and outlook

Deterministic self-assembled QDs has been the candidate for fabricating high fidelity SPSs and entangled photon sources. Due to their high purity, high counting rate and excellent coherence under resonant excitation, these unique quantum light sources can be extensively applied in quantum computation, quantum cryptography, quantum teleportation, quantum storage and so on. The practical single-photon devices inevitably require establishing in an appropriate deterministic QD system that possess super emitting speed, high emitting efficiency, excellent collecting efficiency and completed indistinguishability of single photons. Therefore, incorporating SQDs into optical microcavities, that have high spontaneous emission rate due to the enhanced Purcell effect, renders them to be a very fascinating system for the practical SPSs. Subsequently, we demonstrated the related mechanism of microcavity coupling QDs for enhancing the single-photon emission and certain optical microcavities, such as micropillar, are emphatically investigated. Furthermore, Purcell enhancement of coupled microcavities can increase the indistinguishability of SPSs as well, which is suitable to match the spontaneous emission rate enhancement to the optimum value for high indistinguishability<sup>[21]</sup>. Additionally, we discussed several single-photon devices of  $\text{In}(\text{Ga})\text{As}$  QD semiconductors and focused on investigating the related the growth of QD materials, emitting regimes, properties and so on.

Ultimately, it is important to resolve the following aspects of QD materials and devices for future developments. Firstly, there is need to purify the surrounding environment of single QDs in order to reduce the jitter of QD spectrum and enhancing the high symmetry QDs, which, in turn, can reduce FSS. Secondly, mastering the precise locating technologies will aid realization of the alignment between the micro-cavity and the single QDs besides with the fiber core for enhancing the excited and collected efficiency of single photons. Thirdly, there is a demand to develop the complex structure of active microcavities and the passive waveguides that are suitable for the

generation and manipulation of on-chip isotropic single photons, which can be used in HBT meet/Hong-Ou-Mandel interference tests. Furthermore, there is still need to research the integrated quantum chips of high-transmittance waveguide splitters and Mach-Zender interferometers. All above-mentioned significant researches will afford the developments for improving the single-photon extraction efficiency of micro-cavity, the collection efficiency of light path and the coincident accounting rates.

## Acknowledgments

This work was supported by the National Key Technologies R&D Program of China (Grant No. 2018YFA0306101), the Key R&D Program of Guangdong Province (Grant No. 2018B030329001), the Scientific instrument developing project of the Chinese Academy of Science (Grant No. YJKYYQ20170032), and the National Natural Science Foundation of China (Grant No. 61505196). This work was partly supported by Dr. Xiulai Xu from Beijing National Laboratory for Condensed Matter Physics, Institute of Physics, Chinese Academy of Sciences. We also acknowledged Dr. Xiumei Wang from Wuhan Institute of Physics and Mathematics Chinese Academy of Sciences for the help of results analysis.

## References

- [1] Schneider C, Rahimi-Iman A, Kim N Y, et al. An electrically pumped polariton laser. *Nature*, 2013, 497(7449), 348
- [2] Pelton M, Santori C, Vuckovic J, et al. Efficient source of single photons: A single quantum dot in a micropost microcavity. *Phys Rev Lett*, 2002, 89(23), 233602
- [3] Yoshie T, Scherer A, Hendrickson J, et al. Vacuum Rabi splitting with a single quantum dot in a photonic crystal nanocavity. *Nature*, 2004, 432(7014), 200
- [4] Peter E, Senellart P, Martrou D, et al. Exciton-photon strong-coupling regime for a single quantum dot embedded in a microcavity. *Phys Rev Lett*, 2005, 95(6), 067401
- [5] Pelton M, Yamamoto Y. Ultralow threshold laser using a single quantum dot and a microsphere cavity. *Phys Rev A*, 1999, 59(3), 2418
- [6] Gerard J M, Gayral B. InAs quantum dots: artificial atoms for solid-state cavity-quantum electrodynamics. *Physica E*, 2001, 9(1), 131
- [7] Hargart F, Roy-Choudhury K, John T, et al. Probing different regimes of strong field light-matter interaction with semiconductor quantum dots and few cavity photons. *New J Phys*, 2016, 18, 123031
- [8] Liao S K, Cai W Q, Liu W Y, et al. Satellite-to-ground quantum key distribution. *Nature*, 2017, 549(7670), 43
- [9] Harrow A W, Montanaro A. Quantum computational supremacy. *Nature*, 2017, 549(7671), 203
- [10] Ren J G, Xu P, Yong H L, et al. Ground-to-satellite quantum teleportation. *Nature*, 2017, 549(7670), 70
- [11] Knill E, Laflamme R, Milburn G J. A scheme for efficient quantum computation with linear optics. *Nature*, 2001, 409(6816), 46
- [12] Divincenzo D P. Quantum computation. *Science*, 1995, 270(5234), 255
- [13] Ekert A K. Quantum cryptography based on Bell's theorem. *Phys Rev Lett*, 1991, 67(6), 661
- [14] Gisin N, Ribordy G G, Tittel W, et al. Quantum cryptography. *Rev Mod Phys*, 2002, 74(1), 145
- [15] Wang X L, Cai X D, Su Z E, et al. Quantum teleportation of multiple degrees of freedom of a single photon. *Nature*, 2015, 518(7540), 516
- [16] Gisin N, Thew R. Quantum communication. *Nat Photonics*, 2007, 1(3), 165
- [17] Oxborrow M, Sinclair A G. Single-photon sources. *Contemp Phys*, 2005, 46(3), 173
- [18] Muller A, Herzog T, Huttner B, et al. "Plug and play" systems for quantum cryptography. *Appl Phys Lett*, 1997, 70(7), 793
- [19] Brassard G, Lütkenhaus N, Mor T, et al. Limitations on practical quantum cryptography. *Phys Rev Lett*, 2000, 85(6), 1330
- [20] Yao P J, Rao V, Hughes S. On-chip single photon sources using planar photonic crystals and single quantum dots. *Laser Photon Rev*, 2010, 4(4), 499
- [21] Shan G C, Yin Z Q, Shek C H, et al. Single photon sources with single semiconductor quantum dots. *Front Phys*, 2014, 9(2), 170
- [22] Lounis B, Moerner W E. Single photons on demand from a single molecule at room temperature. *Nature*, 2000, 407(6803), 491
- [23] Keller M, Lange B, Hayasaka K, et al. Continuous generation of single photons with controlled waveform in an ion-trap cavity system. *Nature*, 2004, 431(7012), 1075
- [24] Kuhn A, Hennrich M, Rempe G. Deterministic single-photon source for distributed quantum networking. *Phys Rev Lett*, 2002, 89(6), 4
- [25] Kurtsiefer C, Mayer S, Zarda P, et al. Stable solid-state source of single photons. *Phys Rev Lett*, 2000, 85(2), 290
- [26] Liang B L, Wang Z M, Wang X Y, et al. Energy transfer within ultra-low density twin InAs quantum dots grown by droplet epitaxy. *ACS Nano*, 2008, 2(11), 2219
- [27] He Y M, He Y, Wei Y J, et al. On-demand semiconductor single-photon source with near-unity indistinguishability. *Nat Nanotechnol*, 2013, 8(3), 213
- [28] Badolato A, Hennessy K, Atature M, et al. Deterministic coupling of single quantum dots to single nanocavity modes. *Science*, 2005, 308(5725), 1158
- [29] Aharonovich I, Englund D, Toth M. Solid-state single-photon emitters. *Nat Photonics*, 2016, 10(10), 631
- [30] Chen Y, Zhang J X, Zopf M, et al. Wavelength-tunable entangled photons from silicon-integrated III-V quantum dots. *Nat Commun*, 2016, 7, 10387
- [31] Yu Y, Shang X J, Li M F, et al. Single InAs quantum dot coupled to different "environments" in one wafer for quantum photonics. *Appl Phys Lett*, 2013, 102(20), 201103
- [32] Brown R H, Twiss R Q. Correlation between photons in two coherent beams of light. *Nature*, 1956, 177(4497), 27
- [33] Michler P, Kiraz A, Becher C, et al. A quantum dot single-photon turnstile device. *Science*, 2000, 290(5500), 2282
- [34] Mar J D, Xu X L, Baumberg J J, et al. Bias-controlled single-electron charging of a self-assembled quantum dot in a two-dimensional-electron-gas-based n-i-Schottky diode. *Phys Rev B*, 2011, 83(7), 075306
- [35] Warburton R J, Schaflein C, Haft D, et al. Optical emission from a charge-tunable quantum ring. *Nature*, 2000, 405(6789), 926
- [36] Benson O, Santori C, Pelton M, et al. Regulated and entangled photons from a single quantum dot. *Phys Rev Lett*, 2000, 84(11), 2513
- [37] Mano T, Watanabe K, Tsukamoto S, et al. Fabrication of InGaAs quantum dots on GaAs(001) by droplet epitaxy. *J Cryst Growth*, 2000, 209(2/3), 504
- [38] Ding X, He Y, Duan Z C, et al. On-demand single photons with high extraction efficiency and near-unity indistinguishability from a resonantly driven quantum dot in a micropillar. *Phys Rev Lett*, 2016, 116(2), 020401
- [39] Yu Y, Dou X M, Wei B, et al. Self-assembled quantum dot structures in a hexagonal nanowire for quantum photonics. *Adv Mater*, 2014, 26(17), 2710
- [40] Xie X M, Xu Q, Shen B Z, et al. InGaAsP/InP micropillar cavities for 1.55  $\mu\text{m}$  quantum-dot single photon sources. 6th Conference on Advances in Optoelectronics and Micro/Nano-Optics, Bristol: IOP

- Publishing Ltd, Bristol, 2017, 844
- [41] Heindel T, Schneider C, Lermer M, et al. Electrically driven quantum dot-micropillar single photon source with 34% overall efficiency. *Appl Phys Lett*, 2010, 96(1), 011107
- [42] Xu T, Zhu N, Xu M Y C, et al. A pillar-array based two-dimensional photonic crystal microcavity. *Appl Phys Lett*, 2009, 94(24), 241110
- [43] Vahala K J. Optical microcavities. *Nature*, 2003, 424(6950), 839
- [44] Javadi A, Mahmoodian S, Sollner I, et al. Numerical modeling of the coupling efficiency of single quantum emitters in photonic-crystal waveguides. *J Opt Soc Am B*, 2018, 35(3), 514
- [45] Ali H, Zhang Y Y, Tang J, et al. High-responsivity photodetection by a self-catalyzed phase-pure p-GaAs nanowire. *Small*, 2018, 14(17), 9
- [46] Ward M B, Farrow T, See P, et al. Electrically driven telecommunication wavelength single-photon source. *Appl Phys Lett*, 2007, 90(6), 063512
- [47] Salter C L, Stevenson R M, Farrer I, et al. An entangled-light-emitting diode. *Nature*, 2010, 465(7298), 594
- [48] Dou X M, Chang X Y, Sun B Q, et al. Single-photon-emitting diode at liquid nitrogen temperature. *Appl Phys Lett*, 2008, 93(10), 101107
- [49] Hargart F, Kessler C A, Schwarzback T, et al. Electrically driven quantum dot single-photon source at 2 GHz excitation repetition rate with ultra-low emission time jitter. *Appl Phys Lett*, 2013, 102(1), 011126
- [50] Gerard J M, Solid-state cavity-quantum electrodynamics with self-assembled quantum dots. In: *Single Quantum Dots: Fundamentals, Applications and New Concepts*. Berlin: Springer-Verlag, 2003, 90, 269
- [51] P Michler. *Single quantum dots: Fundamentals, applications and new concepts*. Berlin Heidelberg: Springer Publishing Company, Incorporated, 2003
- [52] Muller M, Bounouar S, Jons K D, et al. On-demand generation of indistinguishable polarization-entangled photon pairs. *Nat Photonics*, 2014, 8(3), 224
- [53] Wang H, Duan Z C, Li Y H, et al. Near-transform-limited single photons from an efficient solid-state quantum emitter. *Phys Rev Lett*, 2016, 116(21), 213601
- [54] He Y, He Y M, Wei Y J, et al. Indistinguishable tunable single photons emitted by spin-flip raman transitions in InGaAs quantum dots. *Phys Rev Lett*, 2013, 111(23), 237403
- [55] Zhang J X, Zallo E, Hofer B, et al. Electric-field-induced energy tuning of on-demand entangled-photon emission from self-assembled quantum dots. *Nano Lett*, 2017, 17(1), 501
- [56] Chen Z S, Ma B, Shang X J, et al. Bright single-photon source at 1.3  $\mu\text{m}$  based on InAs bilayer quantum dot in micropillar. *Nanoscale Res Lett*, 2017, 12(1), 378
- [57] Ma B, Chen Z S, Wei S H, et al. Single photon extraction from self-assembled quantum dots via stable fiber array coupling. *Appl Phys Lett*, 2017, 110(14), 142104
- [58] Zha G W, Shang X J, Su D, et al. Self-assembly of single "square" quantum rings in gold-free GaAs nanowires. *Nanoscale*, 2014, 6(6), 3190
- [59] Yu Y, Li M F, He J F, et al. Single InAs quantum dot grown at the junction of branched gold-free GaAs nanowire. *Nano Lett*, 2013, 13(4), 1399
- [60] Zha G W, Shang X J, Ni H Q, et al. In situ probing and integration of single self-assembled quantum dots-in-nanowires for quantum photonics. *Nanotechnology*, 2015, 26(38), 385706
- [61] Tang J S, Zhou Z Q, Wang Y T, et al. Storage of multiple single-photon pulses emitted from a quantum dot in a solid-state quantum memory. *Nat Commun*, 2015, 6, 8652
- [62] Konthasinghe K, Peiris M, Yu Y, et al. Field-field and photon-photon correlations of light scattered by two remote two-level InAs quantum dots on the same substrate. *Phys Rev Lett*, 2012, 109(26), 267402
- [63] Konthasinghe K, Walker J, iris, et al. Coherent versus incoherent light scattering from a quantum dot. *Phys Rev B*, 2012, 85(23), 235315
- [64] Peiris M, Konthasinghe K, Yu Y, et al. Bichromatic resonant light scattering from a quantum dot. *Phys Rev B*, 2014, 89(15), 155305
- [65] Chen G, Zou Y, Xu X Y, et al. Experimental test of the state estimation-reversal tradeoff relation in general quantum measurements. *Phys Rev X*, 2014, 4(5), 021043
- [66] Chen G, Zou Y, Zhang W H, et al. Experimental demonstration of a hybrid-quantum-emitter producing individual entangled photon Pairs in the telecom band. *Sci Rep*, 2016, 6, 26680
- [67] Buckley S, Rivoire K, Vuckovic J. Engineered quantum dot single-photon sources. *Rep Prog Phys*, 2012, 75(12), 126503
- [68] Franchi S, Trevisi G, Seravalli L, et al. Quantum dot nanostructures and molecular beam epitaxy. *Prog Cryst Growth Charact Mater*, 2003, 47(2/3), 166
- [69] Purcell E M. Spontaneous emission probabilities at radio frequencies. *Phys Rev*, 1946, 69, 681
- [70] Bozhevolnyi S I, Khurgin J B. Fundamental limitations in spontaneous emission rate of single-photon sources. *Optica*, 2016, 3(12), 1418
- [71] Zhao Y P, Li C C, Chen M M, et al. Growth of aligned ZnO nanowires via modified atmospheric pressure chemical vapor deposition. *Phys Lett A*, 2016, 380(47), 3993
- [72] Shang X J, Xu J X, Ma B, et al. Proper In deposition amount for on-demand epitaxy of InAs/GaAs single quantum dots. *Chin Phys B*, 2016, 25(10), 107805
- [73] Zhou P Y, Dou X M, Wu X F, et al. Single-photon property characterization of 1.3  $\mu\text{m}$  emissions from InAs/GaAs quantum dots using silicon avalanche photodiodes. *Sci Rep*, 2014, 4, 3633
- [74] Michler P, Kiraz A, Zhang L D, et al. Laser emission from quantum dots in microdisk structures. *Appl Phys Lett*, 2000, 77(2), 184
- [75] Benson O. Assembly of hybrid photonic architectures from nanophotonic constituents. *Nature*, 2011, 480(7376), 193
- [76] Chen Z S, Ma B, Shang X J, et al. Telecommunication wavelength-band single-photon emission from single large InAs quantum dots nucleated on low-density seed quantum dots. *Nanoscale Res Lett*, 2016, 11(1), 382